Universal Control Strategy using Operating Point Projection Technique for Solar Array Hardware Emulation

Thusitha Randima Wellawatta, Sung-Jin Choi
School of Electrical Engineering
University of Ulsan
Ulsan, South Korea
trwellawatta@gmail.com, sjchoi@ulsan.ac.kr

***Abstract*— Solar array simulator (SAS) is a special DC power supply that regulates the output voltage or current to emulate characteristics of photovoltaic (PV) panels. Especially, the control of SAS is a challenging task due to the nonlinearity in the output curve, which is dependent on irradiance as well as temperature and is determined by panel materials. Conventionally, both current-mode control and voltage-mode control should be alternated by partitioning the operating curve into multiple sections, which is not only for the measurement noise problem with the feedback sensing but also for the control stability issue near the maximum power point. However, the occurrence of transition among different controllers may deteriorate the overall performance. To eliminate the mode transitions, a novel single controller scheme has been introduced in this paper, where the operating point projection technique enables simple, smooth and numerically stable control. Theoretical consideration on the loop stability issue is discussed and the performance is verified experimentally for the emulation of a PV panel data in view of stability and response speed.**

Keywords*— *Solar power, Solar array simulator, Photovoltaic systems, Feedback control

I. INTRODUCTION

Since atmospheric conditions cannot be manipulated, it is usually difficult to conduct controlled experiments with real solar panels. Instead, a hardware equipment called a solar array simulator (SAS) is becoming popular in emulating characteristics of photovoltaic (PV) panels under various irradiance and temperature profiles. SAS is so flexible equipment that researchers can test solar power generation system by feeding sequences of pre-programmed environmental conditions into it. Furthermore, experiments can be repeatable without limitations in time and space. With an updated panel database, different types of panel can also be tested easily.

Basic block diagram of SAS is shown in Fig. 1. It consists of a power converter, a SAS controller, and a SAS engine. The SAS engine generates the target control reference according to the panel data and atmospheric conditions. The SAS controller regulates the output voltage or current of the power converter, which delivers the output power to the load system such as a solar power inverter or battery charger.

The SAS engine contains panel data as a lookup table (LUT) shown in Fig.2. For example, this table can generate a voltage reference, V_{ref}, for the voltage mode controller based on the sensed output current, I_{sense}. In the curve

This work was supported by the National Research Foundation of Korea (NRF) grant funded by the Korea government (MSIP) (No.2017R1A2B4005488).

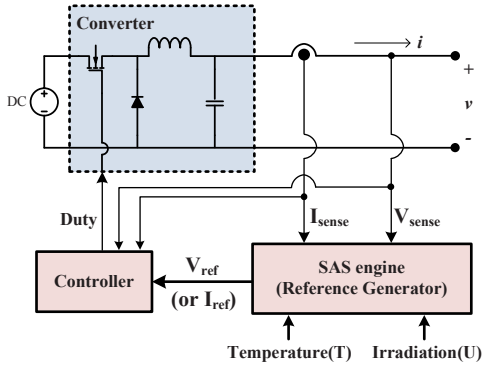

Fig.1 Solar Array Simulator

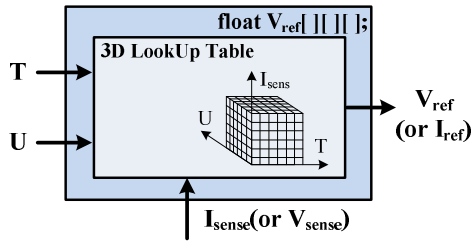

Fig.2 Lookup-Table (LUT) based Solar Array Simulator Engine

generation, the atmospheric information such as temperature, T, and irradiance, U, is also necessary, so three-dimensional table should be considered.

Eventually, the power stage is controlled by the set value of the simulator engine. According to physical properties of a photovoltaic cell, the shape of the I-V characteristic curve of the photovoltaic panel is non-linear as shown in Fig.3. To emulate the curve, current mode control [1], or voltage mode control [2] has been used in the conventional works. In case of current mode control, the current reference is generated from a LUT or model-based control that maps from the sensed voltage, V_{sense}, to the reference current, I_{ref}, but the functionality is limited to the current source segment shown in Fig.3. The similar limitation confines voltage mode control to voltage source segment. In the literature [3], a graphical slope calculation predicts possible instability problems in the vicinity of the maximum power point (MPP) of the I-V curve for voltage mode as well as current mode control. Thus, method has poor performance in the vicinity of MPP.

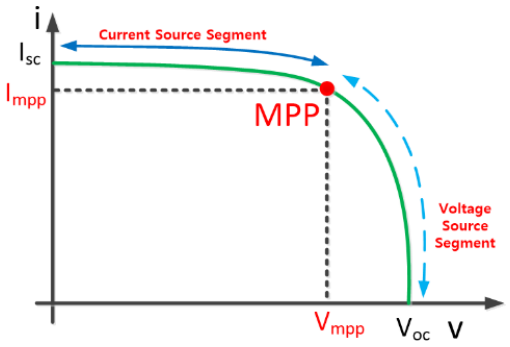

Fig.3 Photovoltaic I-V Characteristic Curve

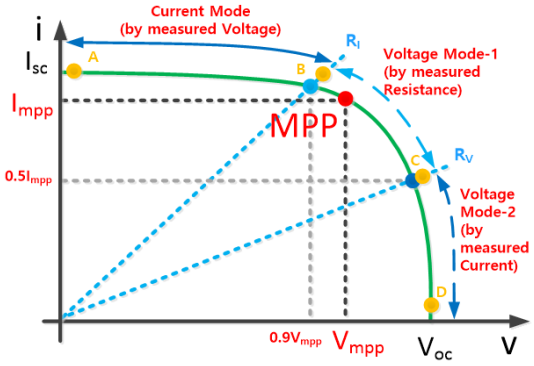

Fig.4 Lookup-Table (LUT) based Solar Array Simulator Engine

As a solution, the hybrid control scheme is presented in the literature [3],[4]. The basic framework of this controller is shown in Fig.4. Here, I-V curve of PV panel is partitioned into three regions. A new region is defined near MPP, where the output is controlled by a voltage mode control, but the reference voltage is calculated by an impedance measured as (1).

$$R_f = \frac{V_{sense}}{I_{sense}} \tag{1}$$

where, V_{sense} and I_{sense} are the sensing values of output voltage and current, respectively. An impedance based algorithm is used in [5] and utilized V-I lookup table with fast dynamic method. However, since the impedance usually becomes either too large in the voltage source segment or too small in the current source segment to cover the entire I-V curve, such a hybrid control or other methods requires multiple controllers to be switched alternately. Thus, fluctuations in the output waveforms due to frequent transitions across the control boundaries may cause another problem. Other algorithms in [6]-[10] discussed about generating the I-V curve by PV model but did not mention about hardware control loop.

The SAS engine contents panel data as a lookup table (LUT) shown in Fig.2. For example, a three-dimensional table can generate a voltage reference, V_{ref}, for the voltage mode controller based on the sensed output current, I_{sense}. In the curve generation, the atmospheric information such as temperature, T, and irradiance, U, is also necessary. Eventually, the power stage is controlled by the set value of the simulator engine. According to physical properties of a photovoltaic cell, the shape of the I-V characteristic curve of the photovoltaic panel is non-linear as shown in Fig.3. To emulate the curve, current mode control, or voltage mode control has been used in the conventional works. In case of current mode control, the current reference is generated from a LUT that maps from the sensed voltage, V_{sense}, to the reference current, I_{ref}, but the functionality is limited to the current source segment shown in Fig.3.

II. Principle of Operation and Proposed Control Scheme

A. Outer loop (reference generator)

According to the above studies, current mode and voltage mode controller are only suitable for the current source section and voltage source section, respectively. It is noticeable that the limitation is originated from the feedback loop gain. In the SAS engine, the control reference signal is generated by the SAS engine, which converts from the sensed signal to the reference signal and it will define the outer feedback loop gain. For example, the outer feedback gain is determined by the incremental slope of the I-to-V conversion LUT in the voltage mode control or that of the V-to-I conversion LUT in the current mode control. However, if the feedback gain is extremely increased beyond their operating region as shown in Fig.5(a), the system becomes unstable and shows the poor dynamic response.

Impedance based control [3]-[5] can be a viable solution to alleviate the problem caused by too large outer loop gain. The impedance is defined by the operating point as shown in Fig.5(b). Fig.6 reflects that distinct voltage reference values can be generated according to the impedance of the operating points. However, according to our observation, this method has a practical issue near the open circuit condition. The measured impedance usually becomes too large in the voltage source segment. That means near the open circuit condition, the impedance reaches to extremely large value (near infinity) and thusly the gain defined from the impedance to the voltage reference becomes so large that system stability can be lost.

Our main research object is to develop a universal control scheme that extends the control range to the entire range of I-V curve in a simple and numerically stable manner. Thus, our study answers to this issue by shifting the origin point as shown in Fig.5(c). The formation of the modified impedance R_m is derived using (2).

$$R_m = \frac{V_{sense} + V_{oc}}{I_{sense} + I_{sc}} \tag{2}$$

where, V_{oc} is the open circuit voltage and I_{sc} is the short circuit current in the standard test condition (STC). The shifting by V_{oc} and I_{sc} makes the feedback gain to be confined into a finite region that never become zero or infinity. This technique guarantees appropriate outer feedback gain to have stable operation in the entire I-V curve.

In the proposed scheme, a modified R-to-V conversion LUT is used to generate the reference voltage. The system block diagram and the control block diagram are shown in

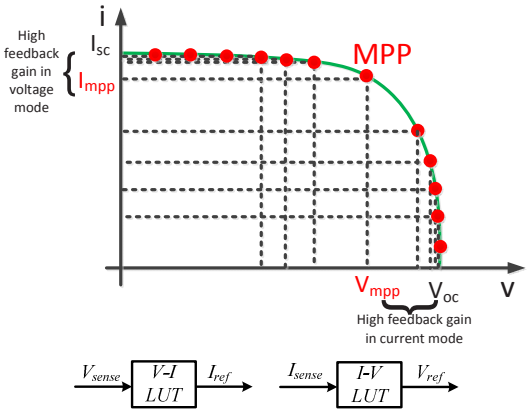

(a) Conventional current/voltage mode control

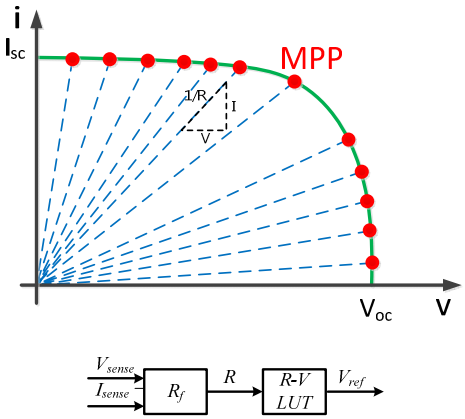

(b) Application of conventional impedance control to the entire region

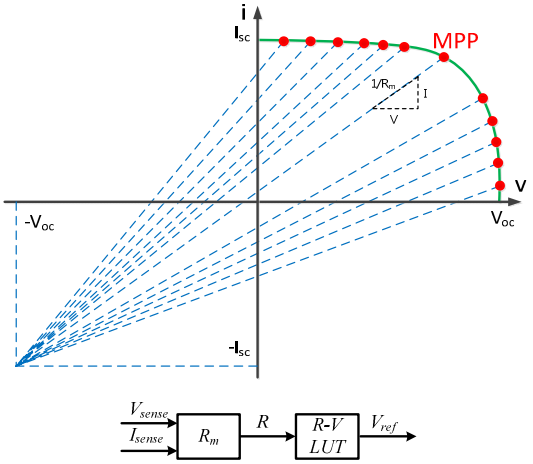

(c) Proposed operating point projection control

Fig.5 Graphical view of control methods

Fig.7. Consequently, the LUT is developed according to the R_m as graphically shown in Fig.8. Transfer functions of voltage and current into resistance and R_m are defined in (3), (4), and (5), respectively.

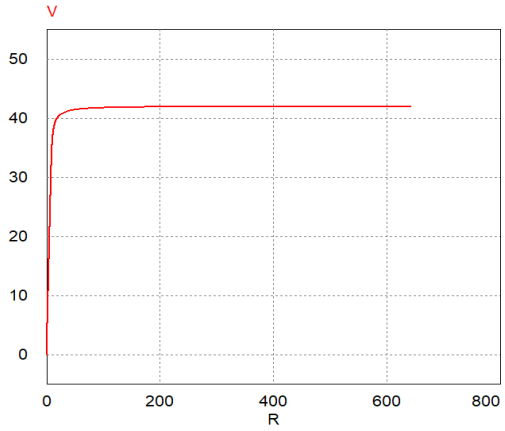

Fig.6 Convectional R to V reference (LUT) curve

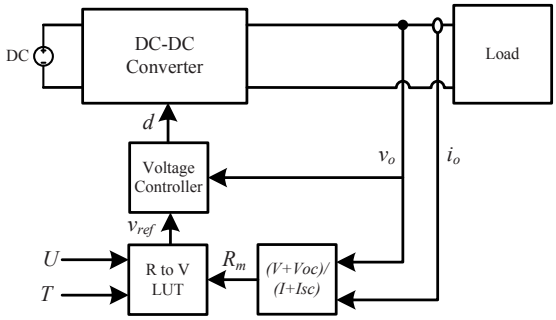

(a) Large signal Block Diagram

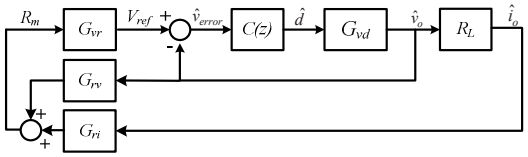

(b) Small signal block diagram

Fig.7 Block Diagram

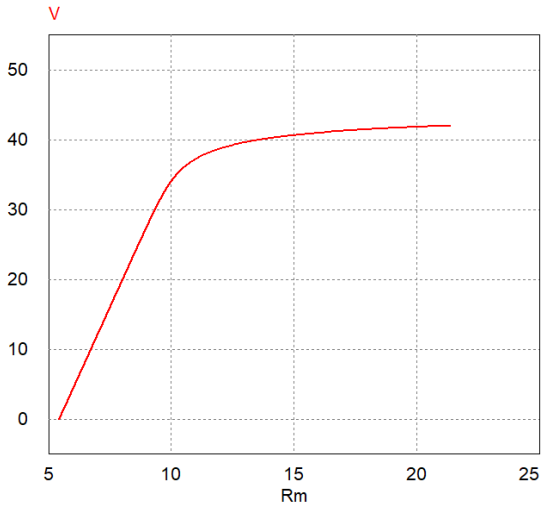

Fig.8 Proposed R_m to V reference (LUT) curve

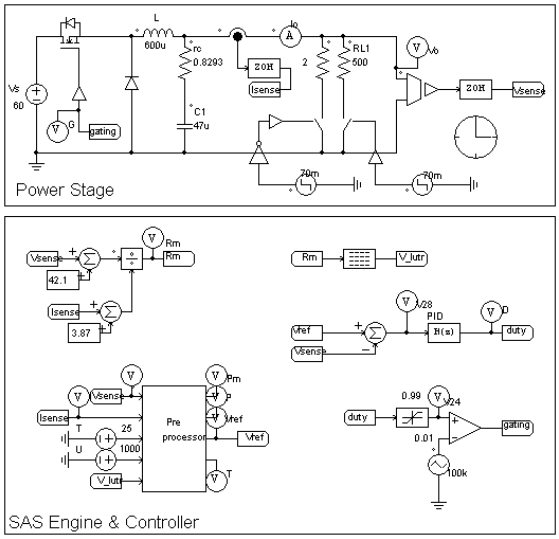

Fig.9 Solar Array Simulator using PSIM

$$G_{rv} = \frac{\hat{r}_m}{\hat{v}_o} \tag{3}$$

$$G_{ri} = \frac{\hat{r}_m}{\hat{i}_o} \tag{4}$$

$$G_{vr} = \frac{\hat{v}_{ref}}{\hat{r}_m} \tag{5}$$

B. Inner loop (output controller)

The voltage transfer function (G_{vd}) of buck converter is derived as (6) by small signal analysis [11]. The compensator can be designed considering the inner voltage loop. The discrete equation of the compensator C(z) is used as (7).

$$G_{vd}(s) = \frac{\hat{v}_O(s)}{\hat{d}(s)} = \frac{v_S}{R_L} \frac{(sCr_C + 1)(R_L + r_C)}{s^2 LC\left(1 + \frac{r_C}{R_L}\right) + s\left(Cr_C + \frac{L}{R_L}\right) + 1} \tag{6}$$

$$C(z) = \frac{b_0 + b_1 z^{-1} + b_2 z^{-2}}{1 + a_1 z^{-1} + a_2 z^{-2}} \tag{7}$$

III. Simulation Results

In the simulation, the conventional method and proposed method are tested and compared on PSIM. The compensators are implemented as Table 1 for conventional hybrid control and Table 2 for the proposed method. The system specifications are shown in Table 3 and tested on 1000W/m^2 insolation and 25^{0}C temperature. The schematic as shown in Fig.9 is used in the simulation and different loads are changed in every 70 milliseconds in PSIM. The simulation waveforms of the output voltage and the output current in conventional system and proposed system in the transition of the load resistance from 12Ω to 40Ωare shown in Fig. 10.

According to the simulation results, proposed method shows more smooth, fast, and stable operation in load transient. Due to control mode switching, conventional method consumes more time to obtain the reference value.

IV. Experiment Results

The experiment is performed with a buck power converter and resistive loads as shown in Fig.11. The SAS controller and SAS engine are implanted in F28377S DSP board. When the load resistance is changed from 12Ω to 40Ω, the waveforms of output voltage and current, and the duty of buck converter are captured and presented in Fig.12. In the experiments, two active loads are parallel connected and activated one after another to obtain the load change.

In the experiment, the output voltage near V_{oc} become more stable than conventional method due to proposed feedback loop. In the load transient, some voltage and current spikes are occurred in conventional method due to control mode switching.

A result from experiment and simulation are also summarized in Table 4. The simulation and experiment show a slight difference because of noise. The proposed system settles the output value within 0.2s with suppressed oscillation. These results prove that the proposed scheme tracks I-V curve of the solar panel effectively with high speed and sufficient stability margin.

Table 1. Conventional controller

Controller		Parameter
Sampling frequency		50kHz
Current Mode	Kp	0.17271
	ki	2302.8
Voltage Mode-1	kp	0.1259642
	ki	292.94
Voltage Mode-2	b0	0.303345
	b1	-0.087633
	b2	0.161784
	a1	0
	a2	-1

Table 2. Proposed controller

PID controller		Parameter
Sampling frequency		50kHz
Phase margin		64.6^0
Gain margin		-343dB
Cutoff frequency		3.98kHz
Settling time		759μs
Coefficients of controller	b0	0.31369728
	b1	-0.49367104
	b2	0.18500096
	a1	-1
	a2	0

Table 3. Specification of hardware

Buck Converter		Parameter
Input Voltage		60V
Inductor		600μH
Capacitor		47uF
Capacitor ESR		0.8293Ω
Switching Frequency		100kHz
Referred PV panel (MSX120)	V_{oc}	42.1V
	I_{sc}	3.87A
	V_{mpp}	33.7V
	I_{mpp}	3.56A
	P_{max}	120W

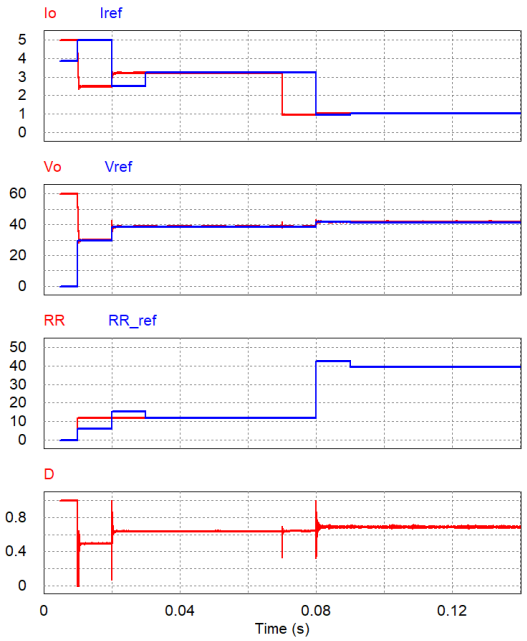

(a) Conventional system

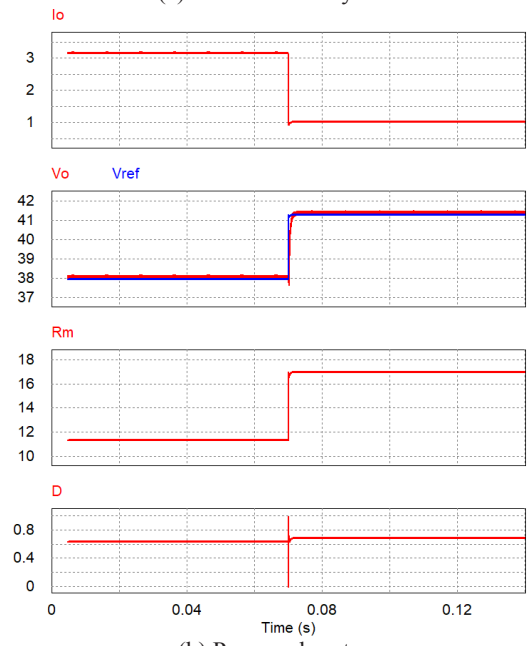

(b) Proposed system

Fig.10 Simulation results (transience of R_L=12Ω → 40Ω)

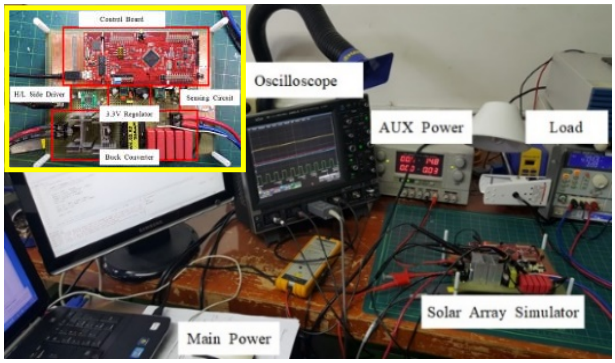

Fig.11 Experimental setup

Table 4. Simulation and experimental results

Output	Data sheet value	Simulation		Experiment	
		Conventional hybrid	Proposed Rm	Conventional hybrid	Proposed Rm
V_o (12Ω)	37.98V	39V	38V	40V	39V
V_o (40Ω)	41.30V	42.9V	41.4V	42.5V	42.0V
I_o (12Ω)	3.16A	3.26A	3.2A	3.5A	3.2A
I_o (40Ω)	1.03A	1.0A	1.0A	1.2A	1.1A

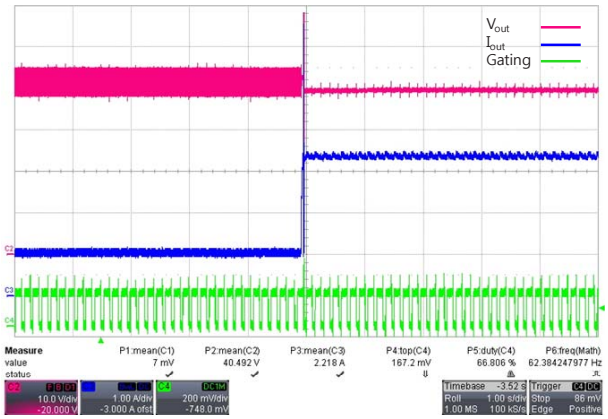

(a) Conventional system

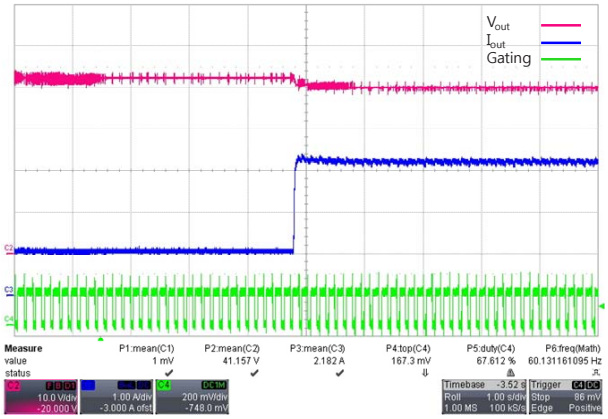

(b) Proposed system

Fig.12 Simulation results (transience of R_L=12Ω → 40Ω)

V. Conclusion

In this paper, a universal control scheme for the solar panel simulator is presented. To solve region-specific stability problem of the conventional works, it utilizes an operating point projection technique to construct a modified R-to-V conversion LUT, which confines the outer feedback loop gain into moderate band. A prototype solar array emulator for a 120W panel is built and tested by the proposed method, where single PID controller covers the entire region of I-V curve. Because this method eliminates the necessity of mode switching between different controller

configurations, it is suitable for high performance solar array simulators that require fast tracking under complex irradiance patterns.

REFERENCES

[1] Ahmed Koran, Kenichiro Sano, Rae-Young Kim and Jih-Sheng Lai, "Design of a Photovoltaic Simulator With a Nobel Reference Signal Generator and Two-Stage LC Output Filter," IEEE Transactions on Power Electronics, Vol.25, NO.5, May.2010

[2] Shlomo Gadelovits, Moshe Sitbon and Alon Kuperman, "Rapid Prototyping of a Low-Cost Solar Array Simulator Using an Off-the-Shelf DC Power Supply," IEEE Transactions on Power Electronics, Vol.29, NO.10, Oct.2014

[3] Y. Li, T. Lee, F. Z. Peng and D. Liu, "A Hybrid Control Strategy for Photovoltaic Simulator," 2009 24th Annual IEEE Applied Power Electronics Conf. and Expo., Washington, DC, 2009, pp. 899-903.

[4] Y.T. Seo, T. Wellawatta, and S.J. Choi "Design and Analysis of 3-Section Hybrid Control Method for Solar Array Simulator," The Transactions of the Korean Institute of Power Electronics, Vol. 23, No. 1, Feb., 2018

[5] I.D.G. Jayawardana, C.N.M. Ho, M. Pokharel, and G. Escobar, "A fast dynamic photovoltaic simulator with instantaneous output impedance matching controller," 2017 IEEE Energy Conversion Congress and Exposition (ECCE), pp.5126 – 5132, 2017

[6] Jun-Young Park and Sung-Jin Choi, "A New PSIM Model for PV Panels Employing Datasheet-based Parameter Tuning," The Transactions of Korea Institute of Power Electronics (KIPE), Vol. 20. No. 6, Dec., 2015.

[7] J.J. Soon and K. S. Low, "Photovoltaic Model Identification Using Particle Swarm Optimization With Inverse Barrier Constraint," IEEE Transactions on Power Electronics, Vol 27, No. 9, Sept., 2012.

[8] D. Sera, R. Teodorescu, and P. Rodriguez, "PV Panel Model Based on Datasheet Values," IEEE International Symposium on Industrial Electronics, pp. 2392-2396, 2007.

[9] B.Chitti Babu and Suresh Gurjar, "A Novel Simplified Two-Diode Model of Photovoltaic(PV) Module," IEEE Journal of Photovoltaics Vol.4, NO.4, July.2014

[10] A.Vijayakumari, A.T.Devarajan and N.Devarajan, "Design and development of a model-based hardware simulator for photovoltaic array," Electrical Power & Energy Systems, 43(2012), p.40-46

[11] ByungCho Choi, Pulsewidth Modulated DC-to-DC Power Conversion Circuit, Dynamics, and Control Designs, WILEY, 2013.